Physica D 272 (2014) 26–38

Contents lists available at ScienceDirect

Physica D

journal homepage: www.elsevier.com/locate/physd

PBC-based pulse stabilization of periodic orbits

Eduardo Liz [a], Christian Pötzsche [b,*]

[a] Departamento de Matemática Aplicada II, Universidade de Vigo, 36310 Vigo, Spain

[b] Institut für Mathematik, Alpen-Adria Universität Klagenfurt, 9020 Klagenfurt, Austria

HIGHLIGHTS

- We give a rigorous approach to periodic control of periodic discrete systems.
- Stability domains help to choose a suitable control for every particular application.
- Destabilizing bifurcations are prevented.
- We give applications for biological and physical models.

ARTICLE INFO

Article history:
Received 5 September 2013
Received in revised form
9 December 2013
Accepted 14 January 2014
Available online 31 January 2014
Communicated by I. Melbourne

Keywords:
Pulse stabilization
Control of chaos
Stability
Bifurcation
Periodic solution
Periodic difference equations

ABSTRACT

We investigate prediction based schemes to stabilize periodic solutions to potentially chaotic systems of periodic difference equations using pulses at times being a multiple of the period. By introducing the concept of a *stability domain*, we obtain precise information on the possibility to stabilize given solutions, to avoid destabilizing bifurcations, as well as on the magnitude of the required control.

1. Introduction

We aim to stabilize an ω_1-periodic solution $\xi = (\xi_n)_{n\in\mathbb{N}_0}$ to a difference equation

$$x_{n+1} = f_n(x_n), \tag{1.1}$$

where the right-hand side $f_n : \Omega \to \Omega$ is continuously differentiable and ω_0-periodic, i.e. $f_n = f_{n+\omega_0}$ for all $n \in \mathbb{N}_0$, and $\Omega \subseteq \mathbb{R}^d$ is an open and nonempty subset. In general, this stabilization is based on a control scheme

$$x_{n+1} = F_n(x_n, u_n), \tag{1.2}$$

with a mapping $F_n : \Omega \times \mathbb{R}^d \to \Omega$ satisfying $F_n(x, 0) = f_n(x)$. Our approach follows two main objectives:

- Given an unstable periodic solution ξ to (1.1) one has the goal to find a control sequence $(u_n)_{n\in\mathbb{N}_0}$ such that ξ becomes an asymptotically stable solution of (1.2), even if ξ is embedded into a possibly chaotic regime.
- More fundamentally in parameter-dependent difference equations (1.1), one tries to choose $(u_n)_{n\in\mathbb{N}_0}$ in a way to avoid the creation of unstable solutions generated by destabilizing bifurcations. This moreover allows to (numerically) continue solutions over larger parameter ranges.

In addition, the control should be as "cheap" as possible in the sense that the control magnitudes are small and controls are applied rarely.

This paper aims to provide a contribution to the control of chaos and targeting, a topic that experiences a fast growth and finds many applications in various areas, including Physics, Chemistry and Biology [1,2]. The main strategies for stabilization of an unstable periodic solution are the so-called feedback methods, which select the perturbation based on the knowledge of the state of the system [3].

* Corresponding author. Tel.: +43 46327003115.
E-mail addresses: eliz@dma.uvigo.es (E. Liz), christian.poetzsche@aau.at (C. Pötzsche).

0167-2789/$ – see front matter
http://dx.doi.org/10.1016/j.physd.2014.01.003

We focus on non-invasive controls, i.e. consider sequences $(u_n)_{n\in\mathbb{N}_0}$ in $\mathbb{R}^d$ and mappings F_n such that ξ is also an ω_1-periodic solution to the controlled difference equation (1.2), instead of creating a new one. A well-known example of these methods is the delayed feedback control (DFC), first established by Pyragas [4]. Our approach is based on prediction-based control (PBC, or predictive control), introduced by Ushio and Yamamoto [5] to overcome some limitations of DFC. This method introduces an external parameter (the *control magnitude*) that helps to stabilization. We intend to provide a general and flexible framework in order to study stability and bifurcations in these control methods, especially when the control is applied in the form of pulses, that is, interventions only take place once every ω_c periods, where $\omega_c \in \mathbb{N}$ is chosen appropriately. This type of pulse control was suggested in several papers [6–9].

Our principle theoretical tool to tackle the above stabilization problem is the concept of a *stability domain*. This subset of the complex plane is characteristic for a particular control scheme and depends on the control magnitude. It indicates whether an unstable solution ξ of (1.1) can be stabilized resp. a bifurcation can be avoided. More precisely, a stabilization is possible, provided there exists a control scheme whose stability domain contains the Floquet spectrum of an unstable solution; a bifurcation can be suppressed as long as the spectrum stays in the stability domain under varying system parameters. We stress that, up to our knowledge, this concept of stability domain is new in the framework of chaos control; it is different from other control domains that search for a parameter region for which a particular system can be stabilized (see, e.g., [10,11]).

Throughout the paper, (asymptotic) stability is always understood in a local sense near the particular reference solution; for global stabilization we refer to [8,12]. The basics of our approach to stabilize periodic solutions to periodic systems of difference equations (1.1) is presented in the subsequent Section 2. Then the following Sections 3–4 discuss external resp. internal prediction based control, the resulting schemes and especially their applicability in preventing destabilizing bifurcations. We close and illustrate our results by means of five explicit examples: A 2-periodic solution to a generalized Beverton–Holt equation can be stabilized over a large parameter domain, whose size certainly depends on the pulse frequency. Afterwards, for each parameter value in the delayed logistic equations we identify minimal control magnitudes required to stabilize the nontrivial fixed point. We are also able to stabilize the Hénon map for a sufficient parameter range, suggest a flexible stabilization scheme for delay-difference equations and finally investigate single-species population models with harvesting.

In order not to interrupt the text, we introduce and discuss various relevant stability domains in the Appendix.

2. Stabilization of periodic solutions

Let us suppose that ω is the least common multiple of both the period ω_1 to the solution $\xi = (\xi_n)_{n\in\mathbb{N}_0}$, as well as to the period ω_0 of the difference equation (1.1). The *period maps* $\pi_n : \Omega \to \Omega$ associated to (1.1) are defined as compositions

$$\pi_n(x) := f_{n+\omega-1} \circ \cdots \circ f_n(x)$$

and one obviously has

$$\pi_n(\xi_n) = \xi_n \quad \text{for all } n \in \mathbb{N}_0. \tag{2.1}$$

We also introduce the *period matrix*

$$\Pi_n(\xi) := f'_{n+\omega-1}(\xi_{n+\omega-1}) \cdots f'_n(\xi_n) \in \mathbb{R}^{d\times d}$$

and it is well-known (see, e.g. [13, Theorem 2.3]) that the periodic solution ξ is asymptotically stable, if and only if all eigenvalues (also called *Floquet multipliers*) of $\Pi_n(\xi)$ are contained in the open unit disk of $\mathbb{C}$. Moreover, provided there exists a Floquet multiplier λ with $|\lambda| > 1$, then ξ is unstable. Note that the Floquet multipliers do not depend on the index $n \in \mathbb{N}_0$ (cf. [13, Proposition 2.2]) and we will typically choose $n = 0$.

In order to stabilize a periodic solution ξ, let us investigate control schemes

$$x_{n+1} = F_n(x_n, u_n(x_n)) \tag{2.2}$$

with a right-hand side $F_n : \Omega \times \mathbb{R}^d \to \Omega$ of class C^1. For the sake of a noninvasive scheme, beyond $F_n(x, 0) = f_n(x)$ we consider continuously differentiable control functions $u : \mathbb{R}^d \to \mathbb{R}^d$ with $u(\xi_0) = 0$. Then a periodic pulse control is realized via

$$u_n(x) = \begin{cases} u(x), & n \in \omega_c\mathbb{N}_0, \\ 0, & n \notin \omega_c\mathbb{N}_0, \end{cases}$$

where ω_c is a multiple of $\omega = \operatorname{lcm}\{\omega_0, \omega_1\}$, say

$$\omega_c = l\omega \quad \text{for some } l \in \mathbb{N}.$$

In doing so, we apply the control in the first step already and wait $\omega_c - 1$ generations until the original difference equation (1.1) is subject to another pulse. The particular integer l indicates the number of cycles after which the control should be applied. In summary, (2.2) is an ω_c-periodic difference equation with linearization

$$\frac{dF_n}{dx}(x, u_n(x)) = \begin{cases} D_1F_n(x, u(x)) + D_2F_n(x, u(x))u'(x), & n \in \omega_c\mathbb{N}_0, \\ f'_n(x), & n \notin \omega_c\mathbb{N}_0. \end{cases}$$

The corresponding period matrix for (2.2) along ξ becomes

$$\tilde{\Pi}_0(\xi) = \Pi_0(\xi)^l + \Pi_0(\xi)^{l-1} f'_{\omega-1}(\xi_{\omega-1}) \cdots f'_1(\xi_1) D_2F_0(\xi_0, 0)u'(\xi_0)$$

and the ω_0-periodic solution ξ is called

- *(locally) stabilizable*, if there exists a $K \in \mathbb{R}^{d\times d}$, so that all eigenvalues of
$$\Pi_0(\xi)^l + \Pi_0(\xi)^{l-1} f'_{\omega-1}(\xi_{\omega-1}) \cdots f'_1(\xi_1) D_2F_0(\xi_0, 0)u'(\xi_0)K \tag{2.3}$$
are contained in the open unit disk $B_1(0) \subseteq \mathbb{C}$
- *(locally) conditionally stabilizable*, provided ξ is (locally) stabilizable by means of the matrix $K = -\alpha I_d$ for some $\alpha \in \mathbb{R}$

The role of the matrix $K \in \mathbb{R}^{d\times d}$ will become clear in the following stability analysis purely based on the linearization of (2.2) along ξ. In fact, K serves as a state feedback or gain state matrix in (2.4) below.

2.1. Stabilization

By means of classical linear control theory (cf. e.g. [14, pp. 429–476, Chapter 10]) one obtains

Proposition 2.1. *If $\Pi_0(\xi)^{l-1} f'_{\omega-1}(\xi_{\omega-1}) \cdots f'_1(\xi_1) D_2F_0(\xi_0, 0)u'(\xi_0) \in \mathbb{R}^{d\times d}$ is invertible, then the periodic solution ξ is locally stabilizable.*

Remark 1. The invertibility assumption is satisfied, if all matrices $D_2F_0(\xi_0, 0)$, $u'(\xi_0)$ and $f'_j(\xi_j)$ for $0 \le j < \omega$ are invertible. In case $l = 1$ it even suffices to assume the latter condition for $1 \le j < \omega$.

Proof. Above all, observe that the periodic solution ξ to (2.2) is asymptotically stable, if and only if the spectrum of $\tilde{\Pi}_0(\xi)$ is contained in the open unit disk $B_1(0) \subseteq \mathbb{C}$, which in turn is equivalent to the asymptotic stability of the linear autonomous equation

$$x_{n+1} = \tilde{\Pi}_0(\xi)x_n = Ax_n + Bx_n \tag{2.4}$$

with the coefficient matrices

$$A := \Pi_0(\xi)^l,$$
$$B := \Pi_0(\xi)^{l-1} f'_{\omega-1}(\xi_{\omega-1}) \cdots f'_1(\xi_1) D_2 F_0(\xi_0, 0) u'(\xi_0).$$

Our invertibility assumption implies $d = \operatorname{rk}(B, AB, A^2B, \dots, A^{d-1}B)$ and consequently [14, p. 433, Theorem 10.4] ensures that the problem $x_{n+1} = Ax_n + Bu_n$ is completely controllable, hence using [14, p. 462, Corollary 10.22] also stabilizable. This means there exists a $K \in \mathbb{R}^{d\times d}$ such that $x_{n+1} = Ax_n + BKx_n$ is asymptotically stable, i.e. the spectrum of $A + BK$ is contained in $B_1(0)$. □

2.2. Conditional stabilization

Often it is too expensive, or hard to realize in vivo, to feedback control (1.1) using a whole matrix $K \in \mathbb{R}^{d\times d}$ as required in (2.3) and one has to restrict to simpler control methods. We actually target at schemes involving only one scalar control parameter, i.e. feedbacks of the form $-\alpha u$, $\alpha \in \mathbb{R}$, rather than Ku. This distinguishes stabilization from conditional stabilization. Here, the *control magnitude* α follows two objectives:

- *Weak control*: α regulates the strength of the control and is preferably of small absolute value.
- *Strong control*: More dynamically, α can be adjusted according to the value of the system parameters in (1.1) in order to oppress destabilizing bifurcations and to continue a given solution over a large parameter range.

For the purpose of a more detailed discussion, suppose there exists a so-called *stability function* $\chi : U \to \mathbb{C}$ on an open domain $U \subseteq \mathbb{C}$, such that one has the representation

$$f'_{\omega-1}(\xi_{\omega-1}) \cdots f'_1(\xi_1) D_2 F_0(\xi_0, 0) u'(\xi_0) = \chi(\Pi_0(\xi_0)). \tag{2.5}$$

Explicit examples that this at first glance rather artificial assumption can be achieved, follow below and thus the linearization (2.3) becomes

$$\Pi_0(\xi)^l - \alpha \Pi_0(\xi)^{l-1} \chi(\Pi_0(\xi)) \in \mathbb{R}^{d\times d}. \tag{2.6}$$

Then we can define the *stability domain*

$$\mathcal{S}^l_\alpha := \{z \in U : |z^l - \alpha z^{l-1}\chi(z)| < 1\} \quad \text{for all } l \in \mathbb{N}$$

of our control scheme (2.2) and illustrate this concept by means of

Example 2.2. Suppose that $\xi \in \Omega$ is an equilibrium of the autonomous equation

$$x_{n+1} = f_0(x_n) \tag{2.7}$$

and let (2.2) be of the form

$$x_{n+1} = f_0(x_n) - \alpha u_n, \qquad u_n(x) := \begin{cases} f_0(x) - x, & n \in l\mathbb{N}_0, \\ 0, & n \notin l\mathbb{N}_0 \end{cases}$$

for some $l \in \mathbb{N}$. Hence, due to $\omega_c = l \operatorname{lcm}\{1, 1\} = l$ the resulting control scheme (2.2) is l-periodic. Thus, (2.6) takes the form

$$f'_0(\xi)^l - \alpha f'_0(\xi)^{l-1}[f'_0(\xi) - I_d] = f'_0(\xi)^l - \alpha f'_0(\xi)^{l-1}\chi(f'_0(\xi))$$

with the stability function $\chi : \mathbb{C} \to \mathbb{C}$, $\chi(z) = z - 1$. This implies the stability domain

$$\begin{aligned} \mathcal{S}^l_\alpha &= \{z \in \mathbb{C} : |z^l - \alpha z^{l-1}(z-1)| < 1\} \\ &= \{z \in \mathbb{C} : |(1-\alpha)z^l + \alpha z^{l-1}| < 1\} \end{aligned}$$

and an analysis of these α-dependent sets for different values of l can be found in the subsequent Examples A.1 and A.2; illustrations are given in Figs. A.13–A.16. For the scalar case, this control scheme has been considered in [8].

Proposition 2.3 (*Properties of the Stability Domain*). *Beyond $\mathcal{S}^l_0 = B_1(0)$ the following holds true for all $l \in \mathbb{N}$ and $\alpha \in \mathbb{R}$:*

(a) *If $z \mapsto z^l - \alpha z^{l-1}\chi(z)$ is continuous, then $\mathcal{S}^l_\alpha$ is open.*
(b) *If $\overline{\chi(z)} = \chi(\bar z)$, then $\mathcal{S}^l_\alpha$ is symmetric w.r.t. the real axis, provided also $U \subseteq \mathbb{C}$ has this property.*
(c) *If $\chi(z) = -\chi(-z)$, then $\mathcal{S}^l_\alpha$ is symmetric w.r.t. the origin, provided also $U \subseteq \mathbb{C}$ has this property.*

When dealing with difference equations (1.1) and (2.2) in $\mathbb{R}^d$ it is important have stability domains fulfilling Proposition 2.3(b), since eigenvalues leave the complex unit disk in complex conjugated pairs.

Proof. Let $z \in \mathcal{S}^l_\alpha$ for $l \in \mathbb{N}$, $\alpha \in \mathbb{R}$.

(a) $\mathcal{S}^l_\alpha$ is the preimage of the open set $(-\infty, 1)$ under a continuous map.
(b) Due to $\left|\bar z^l - \alpha \bar z^{l-1}\chi(\bar z)\right| = \left|\overline{z^l - \alpha z^{l-1}\chi(z)}\right| = \left|z^l - \alpha z^{l-1}\chi(z)\right| < 1$ one has the inclusion $\bar z \in \mathcal{S}^l_\alpha$.
(c) From $(-z)^l - \alpha(-z)^{l-1}\chi(-z) = (-1)^l z^l - \alpha(-1)^l z^{l-1}\chi(z) = (-1)^l[z^l - \alpha z^{l-1}\chi(z)]$ we obtain the desired $-z \in \mathcal{S}^l_\alpha$. □

The terminology "stability domain" is motivated by the following central result:

Theorem 2.4. *Suppose (2.5) holds with a stability function χ holomorphic on U. An ω_1-periodic solution ξ of (1.1) is conditionally stabilizable using a control scheme (2.2), if and only if there exists an $\alpha \in \mathbb{R}$ satisfying the inclusion*

$$\sigma(\Pi_n(\xi)) \subseteq \mathcal{S}^l_\alpha \quad \textit{for one } n \in \mathbb{N}_0.$$

Remark 2. A control scheme (2.2) is called *stability preserving*, if $B_1(0) \subseteq \mathcal{S}^l_\alpha$ holds. This means it does not destabilize asymptotically stable periodic solutions of (1.1) and thus prevents bifurcations caused by a stability change. Actually, it stabilizes Floquet multipliers leaving the complex unit disk, while it has no destabilizing effect on the remaining spectrum. Since for scalar equations (1.1) this remainder of the spectrum is empty, stability preservation is of primary interest when dealing with higher-dimensional problems.

Proof. All period matrices $\Pi_n(\xi)$, $n \in \mathbb{N}_0$, have the same spectrum and therefore we restrict to the case $n = 0$. By definition, the solution ξ is conditionally stabilizable, if and only if (cf. (2.6))

$$\begin{aligned} &|\lambda| < 1 \quad \text{for all } \lambda \in \sigma\left(\Pi_0(\xi)^l - \alpha \Pi_0(\xi)^{l-1}\chi(\Pi_0(\xi))\right) \\ \Leftrightarrow &\left|\lambda^l - \alpha\lambda^{l-1}\chi(\lambda)\right| < 1 \quad \text{for all } \lambda \in \sigma(\Pi_0(\xi)) \\ \Leftrightarrow &\lambda \in \mathcal{S}^l_\alpha \quad \text{for all } \lambda \in \sigma(\Pi_0(\xi)) \end{aligned}$$

due to the spectral mapping theorem (cf., for instance, [15, p. 227, Corollary 1]). □

For later use we also state

Lemma 2.5. *Let ξ be a fixed point of a C^1-mapping $\pi : \Omega \to \Omega$. For $k \in \mathbb{N}$ one has*

(a) *$(\pi^k)'(\xi) = \pi'(\xi)^k$.*
(b) *If π is a C^1-diffeomorphism, then $(\pi^{-k})'(\xi) = \pi'(\xi)^{-k}$.*

Proof. (a) We proceed by mathematical induction. Clearly, the claim holds for $k = 1$. In the induction step $k \to k+1$ we invest $(\pi^k)'(\xi) = \pi'(\xi)^k$, obtain from the chain rule $(\pi^{k+1})'(x) = (\pi \circ \pi^k)'(x) = \pi'(\pi^k(x))(\pi^k)'(x)$ and hence get

$$\begin{aligned} (\pi^{k+1})'(\xi) &= \pi'(\pi^k(\xi))(\pi^k)'(\xi) \\ &= \pi'(\xi)(\pi^k)'(\xi) = \pi'(\xi)^{k+1}. \end{aligned}$$

(b) Since π is a C^1-diffeomorphism, we have $x \equiv \pi^{-1}(\pi(x))$ and differentiation yields by the chain rule $I_d = (\pi^{-1})'(\pi(x))\pi'(x)$. So, $(\pi^{-1})'(\xi)\pi'(\xi) = I_d$ and thus $\pi'(\xi)$ is invertible. Similarly, taking the derivative of the identity $\pi^{-k}(\pi^k(x)) \equiv x$ and setting $x = \xi$ implies the claim (b). □

3. External PBC

This section centers around the concrete control scheme $F_n : \Omega \times \mathbb{R}^d \to \Omega$,

$$F_n(x, u_n) := f_n(x) - \alpha u_n, \tag{3.1}$$

which is clearly noninvasive. Due to $D_2F_n(x, u) = -\alpha I_d$ the period matrix for (2.2) along an ω_1-periodic solution ξ to (1.1) becomes

$$\tilde{\Pi}_0(\xi) = \Pi_0(\xi)^l - \alpha \Pi_0(\xi)^{l-1} f'_{\omega-1}(\xi_{\omega-1}) \cdots f'_1(\xi_1) u'(\xi_0).$$

For prediction based control we choose

$$u_n := u(x_n), \qquad u(x) := \begin{cases} f_0^{\overline{\omega}}(x) - f_0^{\underline{\omega}}(x), & \omega = 1, \\ f'_0(\xi_0)[\pi_0^{\overline{\omega}}(x) - \pi_0^{\underline{\omega}}(x)], & \omega > 1 \end{cases} \tag{3.2}$$

with nonnegative integers $\underline{\omega} < \overline{\omega}$. Provided each $f_n : \Omega \to \Omega$ is a C^1-diffeomorphism, one can additionally allow arbitrary integers $\underline{\omega} < \overline{\omega}$ and in any case Lemma 2.5 implies

$$u'(\xi) = \begin{cases} f'_0(\xi)^{\overline{\omega}} - f'_0(\xi)^{\underline{\omega}}, & \omega = 1, \\ f'_0(\xi_0)[\Pi_0(\xi)^{\overline{\omega}} - \Pi_0(\xi)^{\underline{\omega}}], & \omega > 1. \end{cases}$$

This information and Proposition 2.1 yield conditions for the (local) stabilizability of ξ. On the other hand, to investigate conditional stabilization, we arrive at the stability function

$$\chi(z) := \begin{cases} z^{\overline{\omega}} - z^{\underline{\omega}}, & \omega = 1, \\ z(z^{\overline{\omega}} - z^{\underline{\omega}}), & \omega > 1, \end{cases} \tag{3.3}$$

which is polynomial for $\underline{\omega} \geq 0$. The resulting stability domains of the form

$$\mathcal{S}_\alpha^l \overset{(A.1)}{=} \begin{cases} \mathcal{S}_\alpha^l(l + \overline{\omega} - 1, l + \underline{\omega} - 1), & \omega = 1, \\ \mathcal{S}_\alpha^l(l + \overline{\omega}, l + \underline{\omega}), & \omega > 1 \end{cases} \quad \text{for all } \alpha \neq 1$$

are discussed in the Appendix.

A basic goal of our control approach is to prevent destabilizing bifurcations, which go hand in hand with stability changes caused by Floquet multipliers leaving the unit disk. Thus, it makes sense to restrict to stability preserving schemes.

3.1. Fixed-points of autonomous equations

Let us first investigate fixed points of autonomous equations (1.1), which correspond to the situation $\omega = 1$. Moreover, we focus on the commonly used control

$$u(x) = f_0(x) - x \tag{3.4}$$

(meaning $\overline{\omega} = 1, \underline{\omega} = 0$) yielding the simple stability function $\chi(z) = z - 1$ and the stability domain

$$\mathcal{S}_\alpha^l = \mathcal{S}_\alpha^l(l, l-1).$$

(a) Without pulses ($l = 1$) the corresponding set $\mathcal{S}_\alpha^1(1, 0)$ is discussed in Example A.1; see Figs. A.13 and A.14 for an illustration. This scheme is stability preserving for $\alpha \in (0, 1)$. By choosing the control magnitude α sufficiently close to 1 it is possible to stabilize a fixed point ξ, provided the spectrum $\sigma(f'_0(\xi))$ is either fully contained in the open half-plane $\{z \in \mathbb{C} : \Re z < 1\}$ ($\alpha < 1$), or fully contained in the complementary half-plane $\{z \in \mathbb{C} : \Re z > 1\}$ ($\alpha > 1$). While $\mathcal{S}_\alpha^1(1, 0)$ can be made arbitrarily large, it is not possible to stabilize fixed points with eigenvalues in both of the above half planes, or with real part 1. Yet one can always stabilize fixed points ξ of scalar equations with $f'_0(\xi) \neq 1$.

(b) When introducing pulses ($l > 1$) the stability domains $\mathcal{S}_\alpha^l(l, l-1)$ are considered in Example A.2. While the schemes remain stability preserving for $\alpha \in (0, 1)$, the stability domains drastically shrink (see Figs. A.15 and A.16). Therefore, stabilization can only be expected for spectra near the real axis and moderate imaginary parts.

Both schemes considered in (a) and (b) are stability preserving for $\alpha \in (0, 1)$. However, they have in common that an unstable equilibrium after a transcritical or pitchfork bifurcation, where a simple eigenvalue leaves the unit circle through 1, cannot be stabilized with modest control magnitudes $\alpha \in (0, 1)$ — in fact, it is not possible to stabilize eigenvalues with real part 1. On the other hand, stabilization works for a flip bifurcation, where a simple eigenvalue leaves the unit circle at -1, as well as for a Neimark–Sacker bifurcation. The first situation typically occurs in a period doubling cascade leading to chaotic behavior. However, using the scheme $u(x) = f_0(x) - x$ and allowing $\alpha > 1$ one can avoid a transcritical or pitchfork bifurcation of a scalar equation for $l = 1$. This is also true for pulses with $l = 2$, when one chooses $\alpha > 2$ or $l = 3$ with $\alpha > 3$. Thus, fewer pulses require higher control magnitudes (see Fig. 1).

Next we discuss an external PBC scheme, which somehow circumvents the disadvantage of (a) and (b), namely the fact that eigenvalues with real part 1 cannot be stabilized. Here, we choose

$$u(x) = f_0(x) - f_0^{-1}(x), \tag{3.5}$$

which restricts our considerations to smoothly invertible mappings f_0 and one admittedly looses stability preservation. However, the scheme (3.5) has the benefit that unstable eigenvalues for Eq. (1.1) become stable eigenvalues for the time-reversed system $x_{n+1} = f_0^{-1}(x_n)$ and thus (3.5) incorporates a stabilizing effect. The stability function to (3.5) is $\chi(z) = z - \frac{1}{z}$ and we obtain:

(c) In the absence of pulses, for $l = 1$, one has the stability domain

$$\mathcal{S}_\alpha^1(1, -1) = \{z \in \mathbb{C} \setminus \{0\} : |z - \alpha(z - z^{-1})| < 1\}$$

from Example A.3 illustrated in Figs. A.17 and A.18. It guarantees that a fixed point $\xi \in \Omega$ with arbitrary spectrum $\sigma(f'_0(\xi))$ disjoint from the closed unit disk can be stabilized by choosing $\alpha \in (0, 1)$ sufficiently close to 1 (see Fig. A.17). For parameters $\alpha > 1$ the domain of stability shrinks again, but becomes suitable for real eigenvalues with moduli >1 (see Fig. A.18).

(d) Including pulses, for $l > 1$, the schemes are stability preserving for $\alpha \in (0, 1)$ due to the stability domains

$$\mathcal{S}_\alpha^l(l, l-2) = \{z \in \mathbb{C} : |(1-\alpha)z^l + \alpha z^{l-2}| < 1\} \quad \text{for all } l > 1$$

discussed in Example A.4. Specifically, for $l = 2$ one can stabilize eigenvalues with large imaginary parts (and small real parts) by choosing $\alpha < 1$ close to 1 (for this, cf. Fig. A.19). On the other hand, the situation $1 < \alpha$ stabilizes spectra outside $\bar{B}_1(0)$ featuring eigenvalues with arbitrarily large real parts (and modest imaginary parts, see Fig. A.20).

In summary, for weak controls $\alpha < 1$ only the method without pulses is able to stabilize fixed points of scalar equations after a transcritical, pitchfork or flip bifurcation (in fact for $\alpha = \frac{1}{2}$), where the critical eigenvalues have the value ± 1. With pulses $l > 1$ higher control magnitudes are needed: Bifurcations caused by eigenvalues leaving the unit circle on the real axis require to choose $\alpha > 1$ (at least when $l = 2$) and even larger values of α when $l > 2$ (cf. Fig. 2). However, in two dimensions one can suppress Neimark–Sacker bifurcations for $\alpha < 1$ near 1.

A scheme avoiding also flip bifurcations is given by $u(x) = f_0(x) - f_0^{1-l}(x)$ for odd $l > 2$. With $\alpha \in (0, 1)$ it is stability preserving. The according stability domains are discussed in Example A.5 and illustrated in Figs. A.22 and A.24.

3.2. Nontrivial periodic points

When dealing with nonconstant periodic solutions (or Eqs. (1.1) having period $\omega_0 > 1$) one has a common period $\omega > 1$ and controls apply every ω_cth generation with $\omega_c = l\omega$ for some $l \in \mathbb{N}$. Thus, following (3.3), the stability function becomes

$$\chi(z) = z(z^{\overline{\omega}} - z^{\underline{\omega}})$$

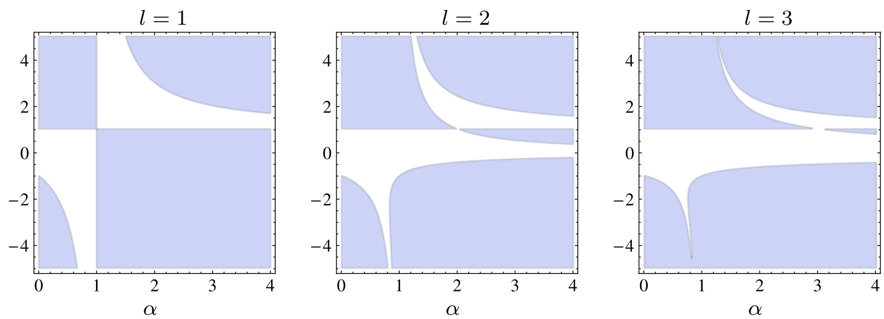

Fig. 1. White shaded areas: Intersection of the stability domain $\mathcal{S}_\alpha^l(l, l-1)$ with the real axis for different values of α (horizontal axis), if $l = 1$ (left), $l = 2$ (center) and $l = 3$ (right).

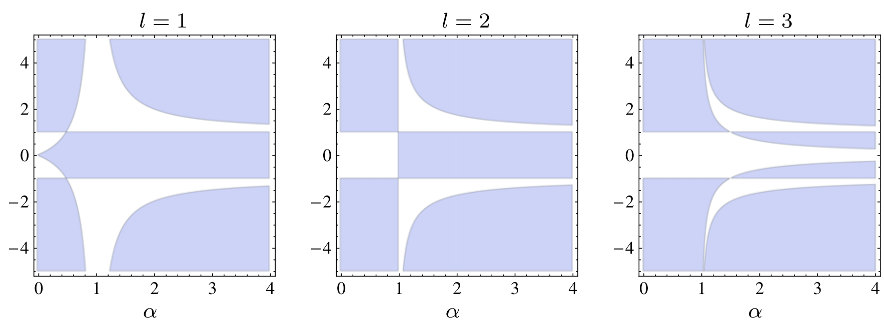

Fig. 2. White shaded areas: Intersection of the stability domain $\mathcal{S}_\alpha^l(l, l-2)$ with the real axis for different values of α (horizontal axis), if $l = 1$ (left), $l = 2$ (center) and $l = 3$ (right).

and moreover implies the stability domains

$$\begin{aligned}\mathcal{S}_\alpha^l &= \{z \in \mathbb{C} : |z^l - \alpha z^l(z^{\overline{\omega}} - z^{\underline{\omega}})| < 1\}\\ &= \mathcal{S}_\alpha^l(l + \overline{\omega}, l + \underline{\omega}) \quad \text{for all } l \in \mathbb{N}.\end{aligned}$$

Therefore one cannot expect stability preserving schemes for all $\alpha \neq 1$.

(a) Without pulses, meaning $l = 1$, a simple control scheme occurs for $\overline{\omega} = 1$, $\underline{\omega} = 0$ yielding the stability domain $\mathcal{S}_\alpha^1(2, 1)$ discussed in Example A.6. Here, for control magnitudes $\alpha < 0$ it is possible to stabilize flip bifurcations. Choosing larger values for $\overline{\omega}$ in $\mathcal{S}_\alpha^1(\overline{\omega} + 1, 1)$ enables to stabilize Floquet multipliers, whose arguments are close to those of the roots of $z^{\overline{\omega}} = -1$. The situation changes when using control magnitudes $\alpha > 0$. In this case, it is possible to stabilize Floquet multipliers leaving the unit circle at the roots of $z^{\overline{\omega}} = 1$.

(b) When applying pulses every lth generation ($l > 1$), the emerging stability domains $\mathcal{S}_\alpha^l(l+\overline{\omega}, l)$ are discussed in Example A.7. One observes that they shrink but behave similarly to the pulse-free situation (a). For instance with $l = 2$, real negative Floquet multipliers can be controlled taking $\overline{\omega} = 1$, imaginary Floquet multipliers taking $\overline{\omega} = 2$ and a triangular symmetry of the stability domain is given for $\overline{\omega} = 3$, etc.

In conclusion, the above schemes to control periodic solutions require small negative values of the parameter α. To avoid bifurcations caused by Floquet multipliers leaving the unit circle at 1, one has to use positive α, where the required control magnitude depends on $\overline{\omega}$ (cf. Fig. 3).

4. Internal PBC

An alternative control scheme $F_n : \mathbb{R}^d \times \mathbb{R}^d \to \mathbb{R}^d$ explicitly reads as

$$F_n(x, u_n) := f_n(x - \alpha u_n) \tag{4.1}$$

and this scheme yields $D_2F_n(x, u) = -\alpha f_n'(x-u)$. The linearization (2.3) becomes

$$\tilde{\Pi}_0(\xi) = \Pi_0(\xi)^l - \alpha\Pi_0(\xi)^l u'(\xi_0).$$

Using the prediction based control

$$u_n := u(x_n), \qquad u(x) := \pi_0^{\overline{\omega}}(x) - \pi_0^{\underline{\omega}}(x)$$

we obtain a noninvasive scheme and employ Lemma 2.5 to arrive at $u'(\xi) = \Pi_0(\xi)^{\overline{\omega}} - \Pi_0(\xi)^{\underline{\omega}}$. Hence, Proposition 2.1 leads to conditions for the (local) stabilizability of ξ.

To investigate conditional stability, we thus have to consider the stability function

$$\chi(z) = z(z^{\overline{\omega}} - z^{\underline{\omega}})$$

and the corresponding stability domains. Their properties are already known from the discussion in the previous Section 3 and the Appendix.

5. Examples

5.1. Generalized Beverton–Holt equation

Let us consider the generalized Beverton–Holt equation

$$x_{n+1} = \frac{\beta x_n}{1 + x_n^\gamma}, \tag{5.1}$$

where $\beta > 0$, $\gamma > 1$ are reals. This difference equation has been very useful in biological models due to its flexibility to fit populations data [16,17]. Differing from the classical Beverton–Holt equation (where $\gamma = 1$), the generalized equation (5.1) with $\gamma > 1$ features a significantly richer dynamics, when the real parameter $\beta > 0$ increases. Let us fix the value $\gamma = 4$, and take β as a bifurcation parameter, that is, we focus on equation

$$x_{n+1} = f_\beta(x_n) := \frac{\beta x_n}{1 + x_n^4}. \tag{5.2}$$

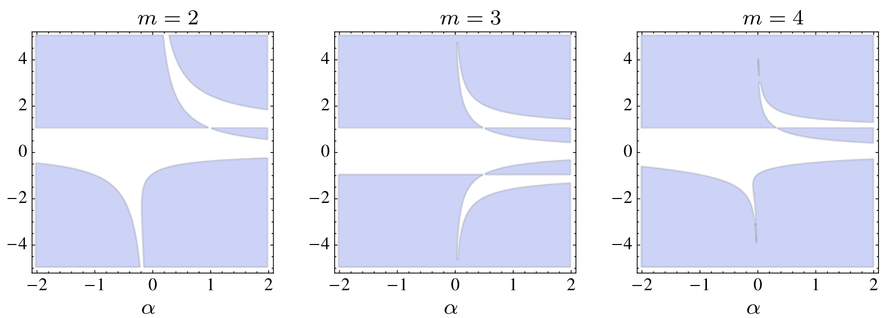

Fig. 3. White shaded areas: Intersection of the stability domain $\mathcal{S}_\alpha^1(m, 1)$ with the real axis for different values of α (horizontal axis), if $m = 2$ (left), $m = 3$ (center) and $m = 4$ (right).

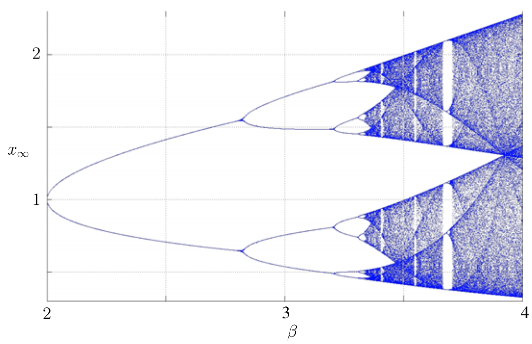

Fig. 4. Feigenbaum diagram illustrating the limit behavior and the period-doubling cascade of the generalized Beverton–Holt equation (5.2) for different values of β (horizontal axis). The symbol x_∞ indicates the long-term behavior (the typical limit set).

For $\beta \in (0, 1]$ the unique equilibrium to (5.2) is the trivial one, until at $\beta = 1$ the asymptotically stable equilibrium $\sqrt[4]{\beta - 1}$ bifurcates.

We are primarily interested in the secondary bifurcation at $\beta = 2$, where $\sqrt[4]{\beta - 1}$ bifurcates into the 2-periodic solution

$$\xi_n := \left(\frac{\beta + \sqrt{\beta^2 - 4}}{2}\right)^{\frac{(-1)^n}{2}} \qquad \text{for all } \beta > 2 \tag{5.3}$$

by means of a flip (period doubling) bifurcation. This solution preserves its asymptotic stability until at $\beta = 2\sqrt{2}$ another flip bifurcation occurs giving rise to an asymptotically stable 4-periodic solution. We depicted the resulting transition into chaotic behavior by means of the Feigenbaum diagram in Fig. 4.

Our intention is to stabilize the 2-periodic solution (5.3) being present for $\beta \geq 2$. Since (5.2) is autonomous (i.e. $\omega_0 = 1$), we have $\omega = 2$. Using external PBC, the control scheme (2.2) becomes explicitly

$$x_{n+1} = \begin{cases} f_\beta(x_n) - \alpha u(x_n), & n \in \omega_c \mathbb{N}_0, \\ f_\beta(x_n), & n \notin \omega_c \mathbb{N}_0 \end{cases} \tag{5.4}$$

with $\omega_c = 2l$ and the control functions (cf. (3.2))

$$u(x) := f_\beta'(\xi_0)(f_\beta^2(x) - x) = -\beta \frac{3\xi_0^4 - 1}{(1 + \xi_0^4)^2} \left(f_\beta^2(x) - x\right).$$

We illustrated the stabilizing behavior by means of the Feigenbaum diagrams in Fig. 5. They indicate that already a moderate control strength $\alpha = -0.1$ yields stabilization for a large interval of values for β — far into the chaotic regime. Clearly, the range for β ensuring that ξ is attractive shrinks when control is only applied every 4th step, i.e. when $\omega_c = 4$ and thus $l = 2$, or even $l = 3$.

Indeed, the decreasing stability domains $\mathcal{S}_{-\alpha}^l(l+1, l)$ (see (A.1)) of the corresponding control schemes for increasing values of $l \in \{1, 2, 3\}$ are illustrated in Fig. 6. Yet, all of them contain the critical eigenvalue -1.

5.2. Delayed logistic equation

In some discrete models, the feedback function involves a delay, leading to a higher order difference equation (or delay-difference equation). Indeed, the dynamics of the delayed logistic equation $x_{n+1} = \lambda x_n(1 - x_{n-k})$ with delay $k \in \mathbb{N}$ is equivalent to the $(k+1)$-dimensional difference equation

$$x_{n+1} = f_\lambda(x_n), \qquad f_\lambda(x) := \begin{pmatrix} \lambda x^1(1 - x^{k+1}) \\ x^1 \\ \vdots \\ x^k \end{pmatrix} \tag{5.5}$$

with right-hand side $f_\lambda : (0, \infty)^{k+1} \to (0, \infty)^{k+1}$ and $\lambda > 0$. Here, the mapping f_λ is invertible, where the inverse becomes

$$f_\lambda^{-1}(x) = \begin{pmatrix} x^2 \\ \vdots \\ x^{k+1} \\ \dfrac{\lambda x^2 - x^1}{\lambda x^2} \end{pmatrix}$$

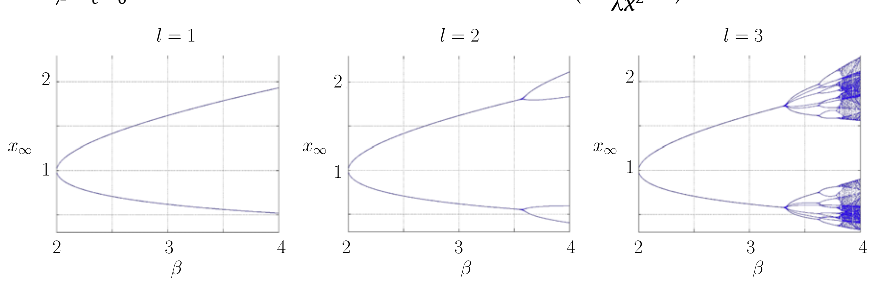

Fig. 5. Feigenbaum diagrams for the external PBC control schemes (5.4) applied to the generalized Beverton–Holt equation (5.2) with $\alpha = -0.1$ and $l = 1$ (left), $l = 2$ (center) and $l = 3$ (right).

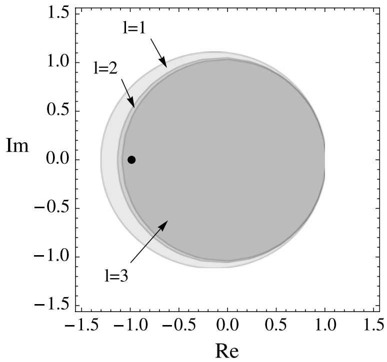

Fig. 6. Critical Floquet multiplier (black dot) and stability domains $\mathcal{S}^l_{-0.1}(l+1,l)$ (gray-shaded areas) for the external PBC schemes (5.4) applied to the generalized Beverton–Holt equation (5.2) with control intensity $\alpha = -0.1$.

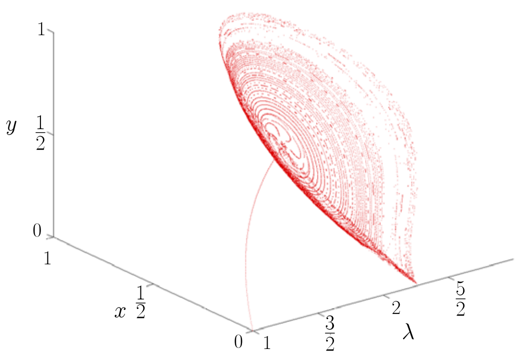

Fig. 7. Bifurcation diagram of the delayed logistic difference equation (5.5) with $k = 1$: Birth of an invariant circle at the parameter value $\lambda = 2$.

and there exist two equilibria

$$\begin{pmatrix}0\\ \vdots\\ 0\end{pmatrix}, \qquad \xi(\lambda) := (1-\tfrac{1}{\lambda})\begin{pmatrix}1\\ \vdots\\ 1\end{pmatrix}$$

to Eq. (5.5). In particular for $k = 1$, the trivial equilibrium loses its asymptotic stability at $\lambda = 1$ and transcritically bifurcates into $\xi(\lambda) \in \mathbb{R}^2$. A secondary bifurcation occurs at $\lambda = 2$, when the asymptotic stability of $\xi(\lambda)$ gets transferred to an invariant circle by means of a Neimark–Sacker bifurcation (see Fig. 7). The corresponding complex-conjugated eigenvalues

$$\mu_\pm(\lambda) := \tfrac{1}{2}(1 \pm \sqrt{5-4\lambda})$$

leave the unit circle for $\lambda = 2$ at the points $\frac{1}{2}\left(1 \pm i\sqrt{3}\right)$.

It turns out that the ability to stabilize the nontrivial equilibrium $\xi(\lambda)$ strongly depends on the delay $k \in \mathbb{N}$. We illustrate this in the following Figs. 8–9. Here, the horizontal axis contains the value of the parameter λ, while the vertical axis indicates the control magnitudes α required to stabilize the nontrivial equilibrium $\xi(\lambda)$ for a particular external PBC scheme (3.1) and pulse frequency $l \in \{1, 2, 3\}$.

- Fig. 8 displays our results for the simplest scheme (3.4), which at least for the delay $k = 1$ is able to stabilize $\xi(\lambda)$ over a large range of λ with modest control magnitudes (cf. Fig. 8 (left)). In Fig. A.13 we depicted the location of the spectrum (delay $k = 1$) w.r.t. the stability domains ($l = 1$). The introduction of pulses drastically lessens the maximal value of λ in which stabilization succeeds to a value between 2 and 2.5.
- To counteract this diminishment, Fig. 9 represents the more advanced scheme (3.5) relying on the inverse of f_λ. Then the introduction of pulses allows a stabilization for large values of λ, provided $k = 1$ (cf. Fig. 9(left)). For delays $k > 1$, the situation becomes more critical. In Fig. A.17 we illustrated the spectrum of the linearization corresponding to $\xi(2)$ and the delay $k = 3$ in relation to the stability domains for different control magnitudes.

5.3. Hénon map

The well-known Hénon map

$$\begin{pmatrix}x_{n+1}\\ y_{n+1}\end{pmatrix} = f_{a,b}(x_n, y_n), \qquad f_{a,b}(x,y) := \begin{pmatrix}y+1-ax^2\\ bx\end{pmatrix} \tag{5.6}$$

with real parameters $a, b > 0$ (the usual choices yielding chaotic behavior are $a = 1.4$ and $b = 0.3$) has the smooth inverse

$$f^{-1}_{a,b}(x,y) = \begin{pmatrix}\dfrac{y}{b}\\ \dfrac{a}{b}y^2 + x - 1\end{pmatrix}.$$

The Eq. (5.6) possesses the two equilibria

$$\xi_\pm(a,b) := \frac{1}{2a}\begin{pmatrix}b-1 \pm \sqrt{4a+(b-1)^2}\\ b(b-1 \pm \sqrt{4a+(b-1)^2})\end{pmatrix},$$

where the corresponding linearizations $f'_{a,b}(\xi_\pm(a,b)) \in \mathbb{R}^{2\times 2}$ typically have eigenvalues in both of the half-planes $\{z \in \mathbb{C} : \Re z < 1\}$ and $\{z \in \mathbb{C} : 1 < \Re z\}$. Hence, a scheme of the form (3.4) will not work (cf. Figs. A.13–A.16).

A possible way to avoid this limitation consists in choosing exponents $m > 1, n = m - 1$ in (A.1) (cf. [18]) and the control scheme

$$u(x) := f^m_{a,b}(x) - f^{m-1}_{a,b}(x).$$

For example, $m = 5, n = 4$ enlarges the region of the pairs (a, b) for which the fixed point $\xi_+(a, b)$ is stabilized with $\alpha = 0.05$; see Fig. 10(left).

Similarly Fig. 10(center, right) illustrates two stability domains for the above scheme being able to stabilize $\xi_+(a, b)$ (choose $m = 5$ and $\alpha = 0.05$), as well as $\xi_-(a, b)$ (choose $m = 4$ and $\alpha = 0.045$).

5.4. Delay-difference equations

We consider a discrete analogue of a model in hematopoiesis (blood cell production) discussed in [19] and [20, Section 4.6]; for further results, see [21,22] and references therein.

This discrete model is defined by a delay-difference equation

$$x_{n+1} = ax_n + (1-a)\frac{b}{1+x^p_{n-k}}, \tag{5.7}$$

where $a \in [0, 1), b > 0, p > 0$ are reals and $k \in \mathbb{N}$. Eq. (5.7) has a unique positive equilibrium $\bar{x}(a, b)$, which is the only positive solution of the equation $x^{p+1} + x = b$.

The dynamics of (5.7) is equivalent to the $(k + 1)$-dimensional difference equation

$$x_{n+1} = f_{a,b}(x_n), \qquad f_{a,b}(x) := \begin{pmatrix}ax^1 + (1-a)g(x^{k+1})\\ x^1\\ \vdots\\ x^k\end{pmatrix}$$

with right-hand side $f_{a,b} : (0,\infty)^{k+1} \to (0,\infty)^{k+1}$, and $g : (0,\infty) \to (0,\infty)$ defined as $g(x) = b/(1 + x^p)$. Since g is strictly monotone, f is invertible. We aim at stabilizing the positive equilibrium $\xi(a, b) = (\bar{x}(a, b), \bar{x}(a, b), \dots, \bar{x}(a, b)) \in (0,\infty)^{k+1}$.

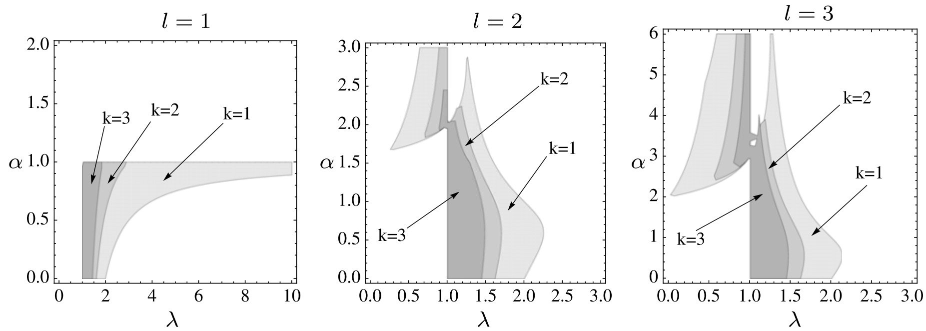

Fig. 8. Gray-shaded areas: Parameter-control pairs (λ, α) for which the simple control scheme (3.4) allows to stabilize the fixed point $\xi(\lambda)$ of (5.5) with control magnitude α and pulse frequencies $l \in \{1, 2, 3\}$ (from left to right) and delays $k \in \{1, 2, 3\}$; notice the different scalings.

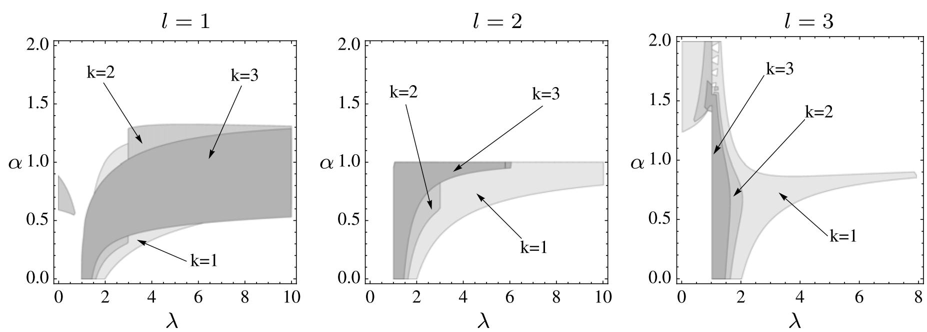

Fig. 9. Gray-shaded areas: Parameter-control pairs (λ, α) for which the control scheme (3.5) allows to stabilize the fixed point $\xi(\lambda)$ of (5.5) with control magnitude α and pulse frequencies $l \in \{1, 2, 3\}$ (from left to right) and delays $k \in \{1, 2, 3\}$; notice the different scalings.

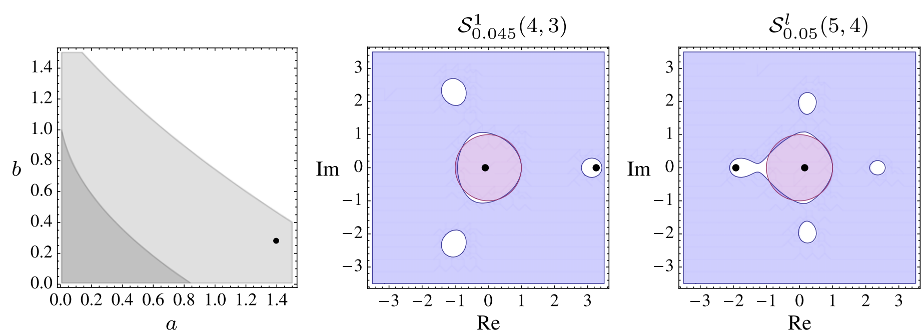

Fig. 10. Left: The gray-shaded areas are parameter pairs (a, b) for which the scheme (3.1)–(3.2) allows to stabilize the fixed point $\xi_+(a, b)$ of (5.6) with parameters $\alpha = 0.05, l = 1$, and $\underline{\omega} = \overline{\omega} - 1$. The small region (in dark gray) corresponds to $\overline{\omega} = 1$, i.e., scheme (3.4), and the large region (in light gray) to $\overline{\omega} = 5$. The latter includes the usual parameter choice $(a, b) = (1.4, 0.3)$ (black dot). Center, right: Eigenvalues (black dots) for the linearization of the Hénon map (5.6) in the equilibria $\xi_-(a, b)$ (center) and $\xi_+(a, b)$ (right) with stability domains $\mathcal{S}^1_{0.045}(4, 3)$ (center) resp. $\mathcal{S}^l_{0.05}(5, 4)$ (right) and the unit disk for schemes stabilizing them (white area).

Let us fix $k = 2, p = 2$. If $b < 2$, the equilibrium $\xi(a, b)$ is asymptotically stable for all $a \in [0, 1)$. In the limit case $a = 0$, the eigenvalues of the linearized equation at $\xi(0, b)$ for $b = 2$ are the cubic roots of -1, and ξ becomes unstable for $b \geq 2$. Actually, at $b = 2$ there is a resonance, leading to the coexistence of two stable periodic solutions (one of period two, and other of period six); for $a > 0$ a Neimark–Sacker bifurcation occurs for a critical value $b^* > 2$, and an invariant curve is born [21,22].

To stabilize $\xi(a, b)$ when $b \geq 2$, we apply the external PBC scheme (3.1) with pulse frequency $l = 3$ and

$$u(x) := f^2_{a,b}(x) - f^{-2}_{a,b}(x). \tag{5.8}$$

The corresponding stability domains $\mathcal{S}^3_\alpha(3, 0)$ are considered in Example A.5; see Fig. A.22. This method fits well to Eq. (5.7); in Fig. 11(left, center) we depict the pairs (a, b) for which the scheme succeeds to stabilize $\xi(a, b)$ with $k = p = 2$ and control magnitudes $\alpha = 0.1$ and $\alpha = 0.2$. Furthermore, Fig. 11(right) illustrates the critical eigenvalues in relation to the stability domains.

5.5. Single-species population models with harvesting

Finally, consider a discrete model for an exploited population. The simplest approach consists of only two processes: reproduction and harvesting. If the population is censused only once (after harvesting or after reproduction), then the resulting model is an autonomous difference equation; however, if the population is monitored twice (after harvesting and after reproduction), then the appropriate mathematical framework is a periodic difference equation [23]. We consider a population with overcompensatory growth defined by the usual Ricker map $f(x) = xe^{r(1-x)}, r > 0$, and subject to constant effort harvesting with harvesting rate $\gamma \in (0, 1)$. The alternation of harvesting and reproduction can be described by the periodic difference equation (1.1), where

$$f_n(x) = \begin{cases} (1-\gamma)x, & n \in 2\mathbb{N}_0, \\ xe^{r(1-x)}, & n \notin 2\mathbb{N}_0, \end{cases} \tag{5.9}$$

whose period map is $\pi_n(x) = f_n((1-\gamma)x) = (1-\gamma)xe^{r(1-(1-\gamma)x)}$.

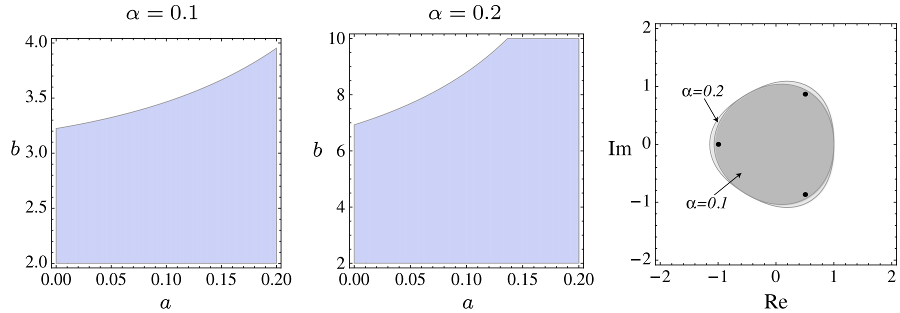

Fig. 11. Left, center: The shaded areas are parameter pairs (a, b) for which the scheme (5.8) with pulse frequency $l = 3$ allows to stabilize the fixed point $\xi(a, b)$ of (5.7) with $k = p = 2$, and magnitudes $\alpha = 0.1$ (left) and $\alpha = 0.2$ (center); notice the different scale in the vertical axis. Right: Stability domains $\mathcal{S}_\alpha^3(3, 0)$ for $\alpha \in \{0.1, 0.2\}$ and the eigenvalues of the linearization along $\xi(a, b)$ with $a = 0.01$ for the critical case $b = 2.02038$.

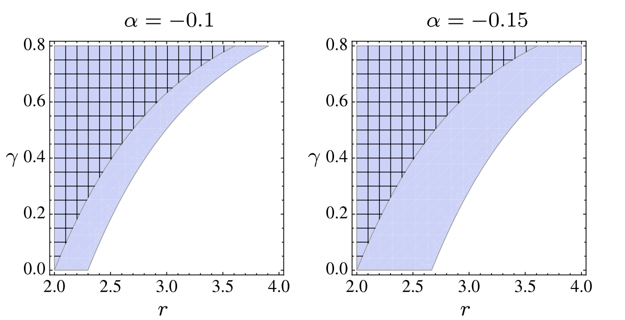

Fig. 12. Blue-shaded areas: Parameter pairs (r, γ) for which the scheme (5.10)–(5.11) allows to stabilize the periodic solution $\xi(r, \gamma)$ of (5.9) with control magnitudes $\alpha = -0.1$ (left) and $\alpha = -0.15$ (right); the meshed region corresponds to pairs for which ξ is asymptotically stable without control.

Denote by $K_{\gamma,r}$ the unique positive solution of $f((1-\gamma)x) = x$, that is,

$$K_{\gamma,r} = \frac{1}{1-\gamma}\left[1 - \frac{1}{r}\ln\left(\frac{1}{1-\gamma}\right)\right],$$

which exists for $0 < \gamma < 1 - e^{-r}$. Then the sequence $\xi(r, \gamma) = (\xi_n)_{n\in\mathbb{N}_0}$ given by $\xi_{2k} = K_{\gamma,r}$, $\xi_{2k+1} = (1-\gamma)K_{\gamma,r}$, $k \in \mathbb{N}_0$, is a 2-periodic solution of (1.1). We aim at stabilizing this solution by a control every time after reproduction, and consequently $\omega_0 = \omega_1 = 2$, $l = 1$.

According to the discussion in Section 3.2, we use the control scheme

$$x_{n+1} = \begin{cases} f_n(x_n) - \alpha u(x_n), & n \in 2\mathbb{N}_0, \\ f_n(x_n), & n \notin 2\mathbb{N}_0 \end{cases} \tag{5.10}$$

with the control functions

$$u(x) := (1-\gamma)(\pi_0(x) - x) = (1-\gamma)\left(f_n((1-\gamma)x) - x\right). \tag{5.11}$$

This control can be interpreted by removing or restocking population depending on the difference between population size after reproduction and the expected population size in the next generation (keeping the same harvesting pressure). The corresponding stability domains are $\mathcal{S}_\alpha^1(2, 1)$, and are considered in Example A.6. Since the 2-periodic solution ξ becomes unstable when its Floquet multiplier is -1, we need to use control magnitudes $\alpha < 0$. It is easy to check that ξ is asymptotically stable if $r \le 2$ or $r > 2$ and $\gamma > 1 - e^{2-r}$.

Fig. 12 shows the pairs (r, γ) for which the scheme succeeds to stabilize $\xi(r, \gamma)$ with control magnitudes $\alpha = -0.1$ and $\alpha = -0.15$.

6. Conclusions

Control of complex dynamics has been one of the main issues in nonlinear science during the last decade [2]. Central problems include the development of new and feasible control schemes, an analytical insight into them, and their applications to interesting areas as biological or technical systems.

In this paper, we further developed prediction-based control schemes for their use in general systems of periodic difference equations, and we provided a rigorous analytic study of stabilization and conditional stabilization of an arbitrary unstable periodic orbit (UPO); the latter allows to control the system using a single scalar control parameter. Compared with the extensive work made for autonomous systems, this particular nonautonomous case has received very little attention, as far as the authors are aware. Nevertheless, in many situations periodic difference equations are more realistic models (for example, for populations growing in a fluctuating habitat [13]). Additionally, dealing with systems also allows to control delay difference equations.

We introduced the concept of a stability domain, which is a very helpful tool to select the more suitable control scheme for each particular application, depending on the location of the Floquet multipliers of the targeted UPO, and to prevent destabilizing bifurcations. Moreover, stability domains are easily computed using the standard computer algebra systems. Our main result establishes that an UPO can be stabilized if there is a control scheme whose stability domain contains its Floquet spectrum. We provide a description of various relevant stability domains for different schemes in the Appendix, and we illustrate their applicability in a number of examples in Section 5.

Our theoretical framework allows pulse stabilization (or periodic feedback [6]). This strategy is particularly useful when control interventions are difficult or costly. Finally, a short program to compute and plot stability domains can be found following the link http://wwwu.uni-klu.ac.at/cpoetzsc/StabilityDomains.nb.

Acknowledgments

E. Liz was supported in part by the Spanish Government and FEDER, grant MTM2010–14837. We thank an anonymous referee for the constructive feedback improving our presentation.

Appendix. Stability domains

For the types of control schemes we were studying, the stability domains $\mathcal{S}_\alpha^l$ can be formulated as

$$\mathcal{S}_\alpha^l(m, n) := \{z \in U : |z^l - \alpha(z^m - z^n)| < 1\} \quad \text{for all } \alpha \neq 1 \tag{A.1}$$

with suitable integers $m > n$ and $l \in \mathbb{N}$. Concerning the domain $U \subseteq \mathbb{C}$ for the stability function χ one chooses $U = \mathbb{C}$ for $n \ge 0$

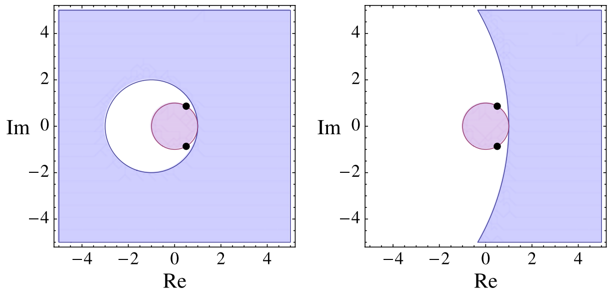

Fig. A.13. Weak control for $\chi(z) = z - 1$: Stability domain $\mathcal{S}_\alpha^1(1, 0)$ (white area) containing the unit disk for magnitudes $\alpha = 0.5$ (left) and $\alpha = 0.9$ (right). The black dots indicate the critical eigenvalue pair for nontrivial solution of the logistic equation (5.5) with $k = 1$.

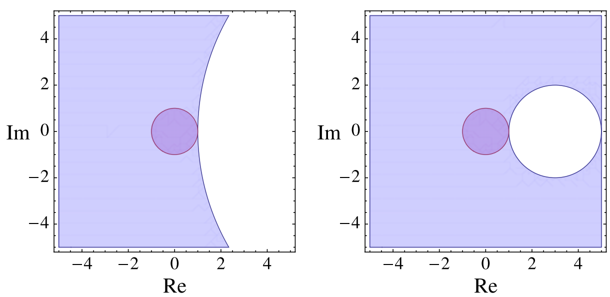

Fig. A.14. Strong control for $\chi(z) = z - 1$: Stability domain $\mathcal{S}_\alpha^1(1, 0)$ (white area) disjoint from the unit disk for magnitudes $\alpha = 1.1$ (left) and $\alpha = 1.5$ (right).

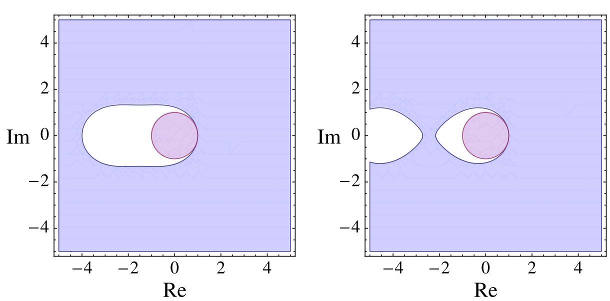

Fig. A.15. Weak control for $\chi(z) = z - 1$: Stability domain $\mathcal{S}_\alpha^2(2, 1)$ (white area) containing the unit disk for magnitudes $\alpha = 0.75$ (left) and $\alpha = 0.83$ (right).

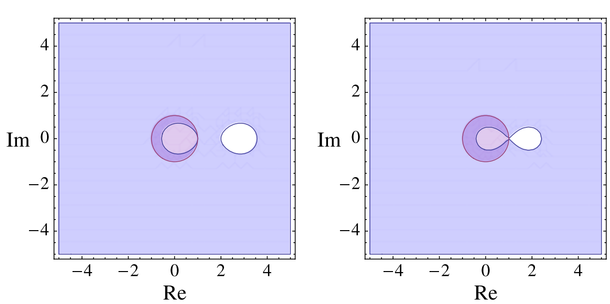

Fig. A.16. Strong control for $\chi(z) = z - 1$: Stability domain $\mathcal{S}_\alpha^2(2, 1)$ (white area) and the unit disk for magnitudes $\alpha = 1.5$ (left) and $\alpha = 2$ (right).

and $U = \mathbb{C} \setminus \{0\}$ otherwise. Moreover, $\mathcal{S}_0^l(m, n) = B_1(0)$ reflects the uncontrolled situation.

We first investigate several properties of these sets for $\alpha \neq 1$. It turns out that $\alpha = 1$ serves as a threshold separating different shapes of $\mathcal{S}_\alpha^l(m, n)$:

(s_0) $1 \in \partial\mathcal{S}_\alpha^l(m, n)$; if both m, n are even (odd), then $-1 \in \partial\mathcal{S}_\alpha^l(m, n)$.

(s_1) *$\mathcal{S}_\alpha^l(m, n)$ is bounded for all $n \geq 0$.*

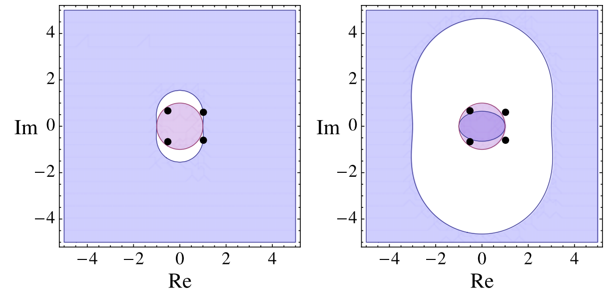

Fig. A.17. Weak control for $\chi(z) = z - \frac{1}{z}$: Stability domain $\mathcal{S}_\alpha^1(1, -1)$ (white area) and the unit disk for magnitudes $\alpha = 0.25$ (left) and $\alpha = 0.75$ (right). The black dots indicate eigenvalues to the linearization along the nontrivial solution of the logistic equation (5.5) with $k = 3$.

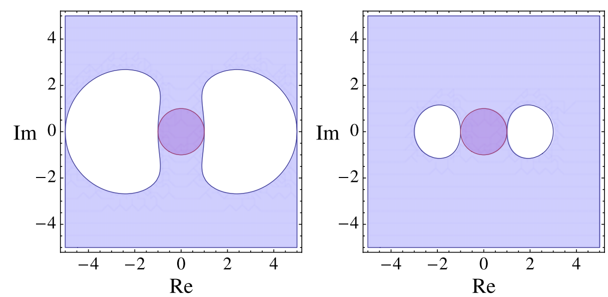

Fig. A.18. Strong control for $\chi(z) = z - \frac{1}{z}$: Stability domain $\mathcal{S}_\alpha^1(1, -1)$ (white area) disjoint from the unit disk for magnitudes $\alpha = 1.25$ (left) and $\alpha = 1.5$ (right).

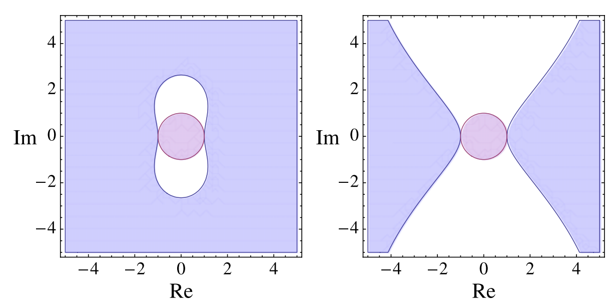

Fig. A.19. Weak control for $\chi(z) = z - \frac{1}{z}$: Stability domain $\mathcal{S}_\alpha^2(2, 0)$ (white area) containing the unit disk for magnitudes $\alpha = 0.75$ (left) and $\alpha = 0.99$ (right).

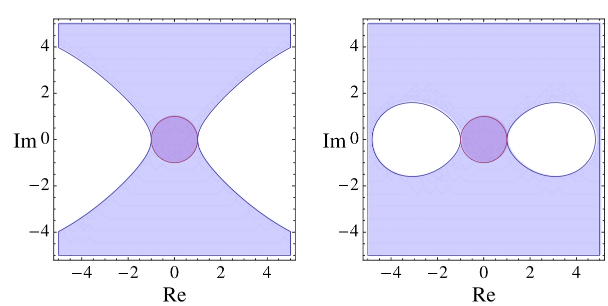

Fig. A.20. Strong control for $\chi(z) = z - \frac{1}{z}$: Stability domain $\mathcal{S}_\alpha^2(2, 0)$ (white area) disjoint from the unit disk for magnitudes $\alpha = 1.01$ (left) and $\alpha = 1.09$ (right).

Proof. Due to $m > n \geq 0$ the function $p(z) := z^l - \alpha(z^m - z^n)$ is a non-constant polynomial. Hence, the assumption that $\mathcal{S}_\alpha^l(m, n)$ is unbounded guarantees that there exists a sequence $(z_n)_{n\in\mathbb{N}}$ in $\mathcal{S}_\alpha^l(m, n)$ such that $\lim_{n\to\infty} |p(z_n)| = \infty$, which contradicts $|p(z_n)| < 1$ for all $n \in \mathbb{N}$.

(s_2) *$\mathcal{S}_\alpha^l(m, n)$ are invariant w.r.t. the rotations $z \mapsto \exp\left(\frac{2\pi}{\gcd\{l,m,n\}} i\right) z$.*

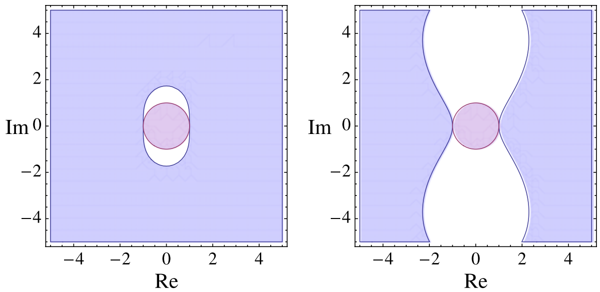

Fig. A.21. Weak control: Stability domain $\mathcal{S}_\alpha^2(2, 0)$ (white area) containing the unit disk for magnitudes $\alpha = 0.5$ (left) and $\alpha = 0.95$ (right).

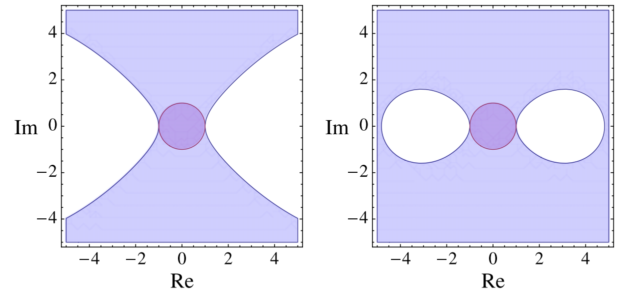

Fig. A.23. Strong control: Stability domain $\mathcal{S}_\alpha^2(2, 0)$ (white area) disjoint from the unit disk for magnitudes $\alpha = 1.01$ (left) and $\alpha = 1.09$ (right).

Proof. Given $z \in \mathcal{S}_\alpha^l(m, n)$ we set $\mu := \gcd\{l, m, n\}$. For $\tilde{z} := e^{2\pi i/\mu} z$ and integers μ_j with $j = \mu\mu_j$ for $j \in \{l, m, n\}$ one has

$$\begin{aligned}|\tilde{z}^l - \alpha(\tilde{z}^m - \tilde{z}^n)| &= |z^l e^{2\mu_l \pi i} - \alpha(e^{2\mu_m \pi i} z^m - e^{2\mu_n \pi i} z^n)| \\ &= |z^l - \alpha(z^m - z^n)| < 1\end{aligned}$$

and consequently $\tilde{z} \in \mathcal{S}_\alpha^l(m, n)$.

(s_3) $B_1(0) \subseteq \mathcal{S}_\alpha^l(m, n)$ *provided* $\alpha \in \begin{cases}(0, 1) \text{ and } l = m > n \geq 0, \\ (-1, 0) \text{ and } m > l = n \geq 0.\end{cases}$

Proof. For every $z \in B_1(0)$ one has

$$|z^l - \alpha(z^l - z^n)| \leq (1 - \alpha)|z^l| + \alpha|z^n| < 1 \quad \text{for all } \alpha \in (0, 1)$$

and therefore $z \in \mathcal{S}_\alpha^l(l, n)$. On the other hand it is

$$|z^l - \alpha(z^m - z^l)| \leq |1 - \alpha z^{m-l} + \alpha| < 1 \quad \text{for all } \alpha \in (-1, 0)$$

if and only if $z^{m-l} \in B_{1/|\alpha|}(\frac{\alpha+1}{\alpha})$. This, nonetheless, holds true because of $z^{m-l} \in B_1(0)$ and $B_1(0) \subseteq B_{1/|\alpha|}(\frac{\alpha+1}{\alpha})$ is satisfied for all $\alpha \in (-1, 0)$.

(s_4) *Let $\zeta_1, \ldots, \zeta_k \in \mathbb{C}$ denote the roots of $z^l - \alpha(z^m - z^n) = 0$ with $n \geq 0$ and $k := \max\{l, m\}$. If all segments $[\zeta_i, \zeta_j]$ are contained in $\mathcal{S}_\alpha^l(m, n)$, then $\mathcal{S}_\alpha^l(m, n)$ is homeomorphic to the open disk $B_1(0)$.*

Proof. First of all, $p(z) := z^l - \alpha(z^m - z^n)$ is a nonconstant polynomial.

We assume that $\mathcal{S}_\alpha^l(m, n)$ is not connected. Due to our assumption, all roots $\zeta_1, \ldots, \zeta_k$ lie in one component and we suppose V is a different component. Then $|p(z)| > 0$ for all $z \in \bar{V}$ and the closed set $\bar{V}$ is bounded, thus compact. Therefore, p has a minimum $p(z^*)$ in $\bar{V}$. On the boundary ∂V it is $|p(z)| \geq 1$, so the minimum must lie in V and satisfy $|p(z^*)| > 0$. By the maximum modulus principle (cf. [24, p. 91, Theorem 1.3]), p is constant on V, which contradicts the fact that p is a nonconstant polynomial. Hence, $\mathcal{S}_\alpha^l(m, n)$ is connected.

Assume that $\mathcal{S}_\alpha^l(m, n)$ is not simply connected. Then the complement has a bounded component U. Since U is closed, $|p(z)|$ achieves its maximum at some $z_0 \in U$. Since the complement $\mathbb{C} \setminus \mathcal{S}_\alpha^l(m, n)$ is closed and U is disjoint from the rest of $\mathbb{C} \setminus \mathcal{S}_\alpha^l(m, n)$, there exists an open ball B which only intersects U. By the choice of z_0 it is

$$\begin{aligned}&|p(z)| < 1 \leq |p(z_0)| \quad \text{for all } z \in B \cap \mathcal{S}_\alpha^l(m, n), \\ &|p(z)| \leq |p(z_0)| \quad \text{for all } z \in B \cap U.\end{aligned}$$

This again contradicts the maximum modulus theorem, since p is not constant. Thus, $\mathcal{S}_\alpha^l(m, n)$ is simply connected. Now the claim follows from the Riemann mapping theorem (see [24, p. 306]).

Unless otherwise noted, the following properties of the stability domains are based on (s_0)–(s_4) and Proposition 2.3:

Example A.1 ($l = m = 1$ *and* $n = 0$)**.** In this simple situation, the stability domain is bounded, topologically connected, symmetric w.r.t. the real axis and explicitly given as

$$\mathcal{S}_\alpha^1(1, 0) = \{z \in \mathbb{C} : |z - \alpha(z - 1)| < 1\} = B_{\frac{1}{|1-\alpha|}}\left(\frac{\alpha}{\alpha - 1}, 0\right).$$

It is the open disk in $\mathbb{C}$ with radius $\frac{1}{|1-\alpha|}$ and center $\left(\frac{\alpha}{\alpha-1}, 0\right)$.

- *Weak control* $\alpha \in (0, 1)$: $\mathcal{S}_\alpha^1(1, 0)$ contains the unit disk $B_1(0)$. By choosing α sufficiently close to 1, $\mathcal{S}_\alpha^1(1, 0)$ contains every bounded subset of the open half-plane $\{z \in \mathbb{C} : \Re z < 1\}$ (cf. Fig. A.13).
- *Strong control* $\alpha > 1$: For α sufficiently close to 1, $\mathcal{S}_\alpha^1(1, 0)$ contains every bounded subset of the open half-plane $\{z \in \mathbb{C} : \Re z > 1\}$ (cf. Fig. A.14).

An introduction of pulses yields shrinking corresponding stability domains, as seen by comparing Figs. A.13, A.14, A.17 and A.18 with for instance the following Figs. A.15 and A.16:

Example A.2 ($m = l > 1$ *and* $n = l - 1$)**.** For $l > 1$ the open stability domains

$$\mathcal{S}_\alpha^l(l, l - 1) = \{z \in \mathbb{C} : |z^l - \alpha z^{l-1}(z - 1)| < 1\}$$

are bounded and symmetric w.r.t. the real axis.

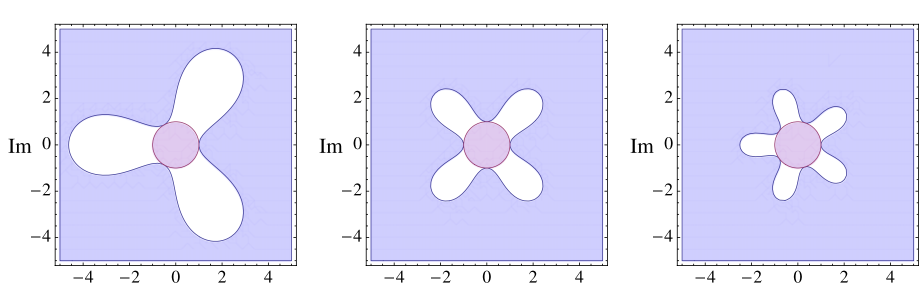

Fig. A.22. Stability domains $\mathcal{S}_{0.98}^l(l, 0)$ (white area) containing the unit disk with $l = 3$ (left), $l = 4$ (center), $l = 5$ (right).

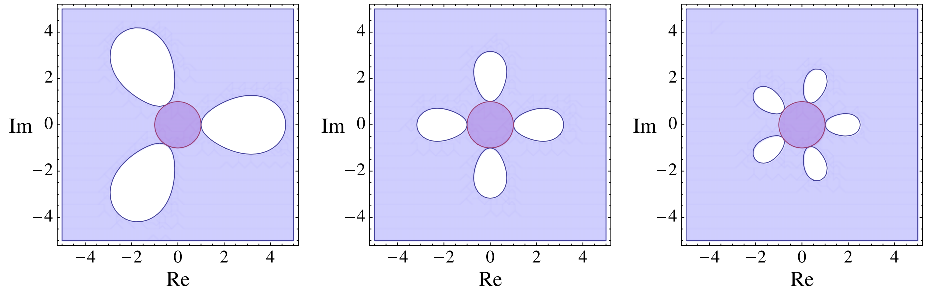

Fig. A.24. Stability domains $\mathcal{S}^l_{1.02}(l,0)$ (white area) and the unit disk with $l=3$ (left), $l=4$ (center) and $l=5$ (right).

- *Weak control* $\alpha\in(0,1)$: The sets $\mathcal{S}^l_\alpha(l,l-1)$ embrace the open unit disk $B_1(0)$. Moreover, since the roots $0, \frac{\alpha}{1-\alpha}$ of $(1-\alpha)z^l+\alpha z^{l-1}$ are contained in the convex set $B_1(0)$, we deduce from (s_4) that $\mathcal{S}^l_\alpha(l,l-1)$ is topologically connected for $\alpha\in(0,\frac{1}{2})$. This fails for certain $\alpha>\frac{1}{2}$, as illustrated in Fig. A.15. For instance, with $l=2$ and concerning the intersection of $\mathcal{S}^2_\alpha(2,1)$ with the real axis, we obtain the maximal inclusions (see Fig. 1(center))

$$\mathcal{S}^2_\alpha(2,1)\supset\begin{cases}\left(\frac{1}{\alpha-1},1\right), & \alpha\in\left(0,2\left(\sqrt{2}-1\right)\right],\\ \left(\frac{1}{\alpha-1},\frac{\alpha-\sqrt{\alpha^2+4\alpha-4}}{2(\alpha-1)}\right)\\ \cup\left(\frac{\alpha+\sqrt{\alpha^2+4\alpha-4}}{2(\alpha-1)},1\right),\\ \alpha\in\left(2\left(\sqrt{2}-1\right),1\right).\end{cases}$$

- *Strong control* $\alpha>1$: For $l=2$ one has (see Figs. A.16 and 1 (center))

$$\mathcal{S}^2_\alpha(2,1)\supset\begin{cases}\left(\frac{\alpha-\sqrt{\alpha^2+4\alpha-4}}{2(\alpha-1)},1\right)\cup\left(\frac{\alpha+\sqrt{\alpha^2+4\alpha-4}}{2(\alpha-1)},\frac{1}{\alpha-1}\right),\\ \alpha\in(1,2],\\ \left(\frac{\alpha-\sqrt{\alpha^2+4\alpha-4}}{2(\alpha-1)},\frac{\alpha+\sqrt{\alpha^2+4\alpha-4}}{2(\alpha-1)}\right)\cup\left(1,\frac{1}{\alpha-1}\right),\\ \alpha\in(2,\infty).\end{cases}$$

The sets $\mathcal{S}^2_\alpha(2,1)$ stay bounded inside a horizontal strip centered around the real axis.

We proceed to a stability domain which is feasible when dealing with smoothly invertible mappings:

Example A.3 ($l=m=1$ *and* $n=-1$)**.** Consider the stability domain

$$\mathcal{S}^1_\alpha(1,-1)=\{z\in\mathbb{C}\setminus\{0\}:\ |z-\alpha(z-z^{-1})|<1\},$$

which is symmetric w.r.t. the real axis and the origin. However, due to the singularity at 0 it cannot contain the unit disk.

- *Weak control* $\alpha\in(0,1)$: One can show the inclusion

$$\left\{z\in\mathbb{C}:\ 1<|z|<\frac{\alpha}{1-\alpha}\right\}\subset\mathcal{S}^1_\alpha(1,-1)\quad\text{for all }\alpha\in\left(\tfrac{1}{2},1\right)$$

and $\mathcal{S}^1_\alpha(1,-1)$ becomes arbitrarily large as $\alpha\nearrow 1$. In fact, for α sufficiently close to 1 the set $\mathcal{S}^1_\alpha(1,-1)$ contains every bounded subset of $\mathbb{C}\setminus\bar{B}_1(0)$ (cf. Fig. A.17). Concerning the intersection with the real axis one has (see Fig. 2(left))

$$\mathcal{S}^1_\alpha(1,-1)\supset\begin{cases}\left(-1,\frac{\alpha}{\alpha-1}\right)\cup\left(\frac{\alpha}{1-\alpha},1\right), & \alpha\in\left(0,\frac{1}{2}\right),\\ \left(\frac{\alpha}{\alpha-1},-1\right)\cup\left(1,\frac{\alpha}{1-\alpha}\right), & \alpha\in\left(\frac{1}{2},1\right)\end{cases}$$

and therefore $\mathcal{S}^1_\alpha(1,-1)$ contains reals with absolute value >1 even for $\alpha<1$.

- *Strong control* $\alpha>1$: One still has the inclusion (cf. Figs. A.18 and 2 (left))

$$\left(\frac{\alpha}{1-\alpha},-1\right)\cup\left(1,\frac{\alpha}{\alpha-1}\right)\subset\mathcal{S}^1_\alpha(1,-1)$$

guaranteeing that $\mathcal{S}^1_\alpha(1,-1)$ grows arbitrarily large for $\alpha\searrow 1$.

Example A.4 ($m=l>1$ *and* $n=l-2$)**.** Given $l>1$, the bounded stability domains

$$\mathcal{S}^l_\alpha(l,l-2)=\{z\in\mathbb{C}:\ |z^l-\alpha z^{l-1}(z-z^{-1})|<1\}$$

are symmetric w.r.t. the real axis and the origin.

- *Weak control* $\alpha\in(0,1)$: $\mathcal{S}^l_\alpha(l,l-2)$ contains the open unit disk. Moreover, the roots of $(1-\alpha)z^2+\alpha=0$ given by $\pm i\sqrt{\frac{\alpha}{\alpha-1}}$ are contained in $B_1(0)$ and for this reason $\mathcal{S}^l_\alpha(l,l-2)$ is connected for $\alpha\in\left(0,\frac{1}{2}\right)$. In particular, one has

$$\left\{iy:\ |y|<\sqrt{\frac{1+\alpha}{1-\alpha}}\right\}\subset\mathcal{S}^2_\alpha(2,0)\quad\text{for all }\alpha\in(0,1)$$

and therefore by choosing α sufficiently close to 1 ($\alpha<1$), every point on the imaginary axis is contained in one $\mathcal{S}^2_\alpha(2,0)$ (see Fig. A.19).

- *Strong control* $\alpha>1$: One has the inclusions

$$\left(-\sqrt{\frac{1+\alpha}{1-\alpha}},-1\right)\cup\left(1,\sqrt{\frac{1+\alpha}{1-\alpha}}\right)\subset\mathcal{S}^2_\alpha(2,0)\quad\text{for all }\alpha>1$$

and for α sufficiently close to 1 ($\alpha>1$), every point of $(-\infty,-1)\cup(1,\infty)$ is contained in one $\mathcal{S}^2_\alpha(2,0)$ (see Figs. A.20 and 2 (center)).

The use of pulses can also yield stability preserving schemes for weak controls:

Example A.5 ($m=l>1$ *and* $n=0$)**.** Here, the open stability domains

$$\mathcal{S}^l_\alpha(l,0)=\{z\in\mathbb{C}:\ |z^l-\alpha z^{l-1}(z-z^{1-l})|<1\}\quad\text{for all }\alpha\neq 1$$

possess a number of interesting symmetry properties: $\mathcal{S}^l_\alpha(l,0)$ is bounded, symmetric w.r.t. the real axis and rotations $\exp(\frac{2\pi}{l}i)$; for even $l\in\mathbb{N}$ the sets $\mathcal{S}^l_\alpha(l,0)$ are also symmetric w.r.t. 0. We deduce that the boundaries $\partial\mathcal{S}^l_\alpha(l,0)$ contain the roots of unity $\exp(\frac{2\pi k}{l}i)$, $0\le k<l$. For an illustration, we refer to Figs. A.21–A.24. In particular, for odd $l>2$ we obtain the inclusion

$$\left(-\sqrt[l]{\frac{1+\alpha}{1-\alpha}},1\right)\subset\mathcal{S}^l_\alpha(l,0)\quad\text{for all }\alpha\in(0,1).$$

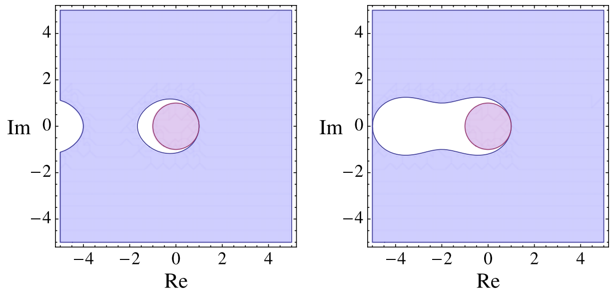

Fig. A.25. Negative control magnitude in Example A.6: Stability domain $\mathcal{S}_\alpha^1(2, 1)$ (white area) and the unit disk for $\alpha = -0.15$ (left) and $\alpha = -0.2$ (right).

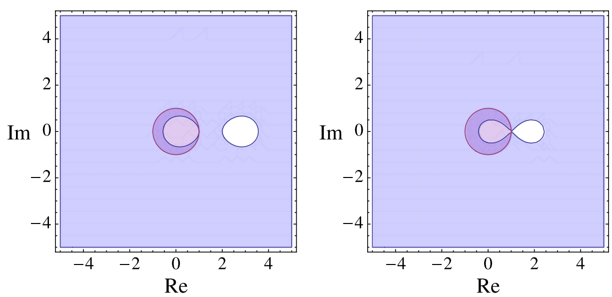

Fig. A.26. Positive control magnitude in Example A.6: Stability domain $\mathcal{S}_\alpha^1(2, 1)$ (white area) and the unit disk for $\alpha = 0.5$ (left) and $\alpha = 0.99$ (right).

- *Weak control* $\alpha \in (0, 1)$: First, $\mathcal{S}_\alpha^l(l, 0)$ contain the open unit disk $B_1(0)$. The sets $\mathcal{S}_\alpha^l(l, 0)$ become topologically connected for $\alpha \in \left(0, \frac{1}{2}\right)$, since the roots of $(1 - \alpha)z^l + \alpha$ lay in $B_1(0)$ (cf. Figs. A.21 and A.22). Furthermore, the stability domains $\mathcal{S}_\alpha^l(l, 0)$ contain the segments
$$\left[0, \sqrt[l]{\tfrac{1+\alpha}{1-\alpha}} \exp\left(\tfrac{2k+1}{l}\pi i\right)\right) \quad \text{for all } \alpha \in (0, 1),\ 0 \le k < l.$$
- *Strong control* $\alpha > 1$: The stability domains are disjoint from the unit disk and disconnected with l components (cf. Figs. A.23 and A.24).

The following stability domains occur when dealing with periodic equations (1.1) and require negative magnitudes for α when aiming at weak control:

Example A.6 ($l = 1, m = 2$ *and* $n = 1$)**.** The open and bounded stability domain
$$\mathcal{S}_\alpha^1(2, 1) = \{z \in \mathbb{C} : |z - \alpha(z^2 - z)| < 1\}$$
is symmetric w.r.t. the real axis. One deduces the maximal inclusions (cf. Fig. 3(left))
$$\mathcal{S}_\alpha^1(2, 1) \supset \begin{cases} \left(\dfrac{1}{\alpha}, 1\right), & \alpha \in \left(-2\sqrt{2} - 3, 2\sqrt{2} - 3\right], \\ \left(\dfrac{1}{\alpha}, \dfrac{1 + \alpha - w}{2\alpha}\right) \cup \left(\dfrac{1 + \alpha + w}{2\alpha}, 1\right), \\ \alpha \in \left(2\sqrt{3} - 3, 0\right) \end{cases}$$
with $w := \sqrt{1 + 6\alpha + \alpha^2}$ and obtains that $B_1(0) \subset \mathcal{S}_\alpha^1(2, 1)$ for $\alpha \in (-1, 0)$ (see Fig. A.25). Because the roots of $z - \alpha(z^2 - z)$ are $0, \frac{1+\alpha}{\alpha}$ and thus contained in $B_1(0)$, we obtain that $\mathcal{S}_\alpha^1(2, 1)$ is connected for $\alpha < -\frac{1}{2}$. On the other hand, the stability domains $\mathcal{S}_\alpha^1(2, 1)$ for control magnitudes $\alpha > 0$ are depicted in Fig. A.26.

Example A.7 ($l = n \in \mathbb{N}, m > l$)**.** Generalizing Example A.6 we see that the open sets
$$\mathcal{S}_\alpha^l(m, l) = \{z \in \mathbb{C} : |z^l - \alpha z^{l-1}(z^{m-l+1} - z)| < 1\}$$
for all $\alpha \neq 1$

are bounded and moreover

- *Weak control* $\alpha \in (-1, 0)$: $\mathcal{S}_\alpha^l(m, l)$ contain the open unit disk by (s_3). Since the roots of $z^l - \alpha(z^m - z^l)$ are either 0 or $(m-l)$th roots of unity to $\frac{\alpha+1}{\alpha}$, they are contained in the convex set $B_1(0)$; thus $\mathcal{S}_\alpha^l(m, l)$ is connected for $\alpha < -\frac{1}{2}$.
- *Strong control*: For $|\alpha| > 1$ one loses the inclusion $B_1(0) \subseteq \mathcal{S}_\alpha^l(m, l)$.

References

[1] W.L. Ditto, M.L. Spano, J.F. Lindner, Techniques for the control of chaos, Physica D 86 (1995) 198–211.
[2] E. Schöll, H.G. Schuster (Eds.), Handbook of Chaos Control, second ed., Wiley-VCH, Weinheim, 2008.
[3] S. Boccaletti, C. Grebogi, Y.C. Lai, H. Mancini, D. Maza, The control of chaos: theory and applications, Phys. Rep. 329 (2000) 103–197.
[4] K. Pyragas, Continuous control of chaos by self-controlling feedback, Phys. Lett. A 170 (1992) 421–428.
[5] T. Ushio, S. Yamamoto, Prediction-based control of chaos, Phys. Lett. A 264 (1999) 30–35.
[6] H.G. Schuster, M.B. Stemmler, Control of chaos by oscillating feedback, Phys. Rev. E 56 (1997) 6410–6417.
[7] Ö. Morgül, On the stabilization of periodic orbits for discrete time chaotic systems, Phys. Lett. A 335 (2005) 127–138.
[8] E. Braverman, E. Liz, Global stabilization of periodic orbits using a proportional feedback control with pulses, Nonlinear Dynam. 67 (2012) 2467–2475.
[9] E. Braverman, E. Liz, On stabilization of equilibria using predictive control with and without pulses, Comput. Math. Appl. 64 (2012) 2192–2201.
[10] K. Pyragas, Control of chaos via an unstable delayed feedback controller, Phys. Rev. Lett. 86 (2001) 2265–2268.
[11] P. Hövel, E. Schöll, Control of unstable steady states by time-delayed feedback methods, Phys. Rev. E 72 (2005) 046203.
[12] E. Liz, D. Franco, Global stabilization of fixed points using predictive control, Chaos 20 (2010) 023124.
[13] C. Pötzsche, Bifurcations in a periodic discrete-time environment, Nonlinear Anal. RWA 14 (2013) 53–82.
[14] S. Elaydi, An Introduction to Difference Equations, third ed., in: Undergraduate Texts in Mathematics, Springer, New York, 2005.
[15] K. Yosida, Functional Analysis, in: Grundlehren der Mathematischen Wissenschaften, vol. 123, Springer, Berlin etc., 1980.
[16] T.S. Bellows, The descriptive properties of some models for density dependence, J. Anim. Ecol. 26 (1981) 139–156.
[17] W.M. Getz, A hypothesis regarding the abruptness of density dependence and the growth rate of populations, Ecology 77 (1996) 2014–2026.
[18] B.T. Polyak, Chaos stabilization by predictive control, Autom. Remote Control 66 (2005) 1791–1804.
[19] G. Karakostas, Ch.G. Philos, Y.G. Sficas, The dynamics of some discrete population models, Nonlinear Anal. 17 (1991) 1069–1084.
[20] V.L. Kocić, G. Ladas, Global Behavior of Nonlinear Difference Equations of Higher Order with Applications, in: Mathematics and its Applications, vol. 256, Kluwer Academic Publishers Group, Dordrecht, 1993.
[21] H.A. El-Morshedy, V. Jiménez López, E. Liz, Periodic points and stability in Clark's delayed recruitment model, Nonlinear Anal. RWA 9 (2008) 776–790.
[22] E. Liz, Global stability and bifurcations in a delayed discrete population model, Int. J. Qual. Theory Differ. Equ. Appl. 3 (2009) 66–80.
[23] F.M. Hilker, E. Liz, Harvesting, census timing and "hidden" hydra effects, Ecol. Complex. 14 (2013) 95–107.
[24] S. Lang, Complex Analysis, fourth ed., in: Graduate Texts in Mathematics, vol. 103, Springer, Heidelberg etc., 1999.